

# One-Dimensional Carbon Nanostructures —From Synthesis to Nano-electromechanical Systems Sensing Applications—

M. A. Fraga,\* R. S. Pessoa,<sup>1</sup> D. C. Barbosa, and V. J. Trava Airoldi

Associate Laboratory of Sensors and Materials, National Institute for Space Research,  
São José dos Campos, SP, 12227-010, Brazil

<sup>1</sup>Nanotechnology and Plasma Processes Laboratory, Universidade do Vale do  
Paraíba, São José dos Campos, SP, 12244-000, Brazil

(Received March 2, 2016; accepted June 2, 2016)

**Keywords:** 1D carbon, nanotube, nanofiber, nanowire, NEMS

The fundamental properties of one-dimensional (1D) carbon nanostructures and their promising technological applications have stimulated significant research in different areas. Because of their outstanding electrical and mechanical properties, these nanostructures have emerged as a new class of sensor material with real potential for a variety of nano-electromechanical systems (NEMS). Several studies have shown that the performance of a NEMS device is significantly affected by the material properties of the nanostructures used to build it. For this reason, a section of this review is devoted to the synthesis and properties of 1D carbon nanostructures including nanotubes, nanofibers, and nanowires. Thereafter, some NEMS-based sensors using 1D carbon nanostructures are introduced and issues related to their fabrication processes are addressed. The goal of this brief review is to outline the benefits of the use of 1D carbon nanostructures, the current status of development and challenges to enable their widespread application as sensing elements in NEMS devices.

## 1. Introduction

Nano-electromechanical systems (NEMS) are devices that integrate electrical and mechanical functionalities on the nanoscale for sensing, actuation, signal processing, display, control and/or interface functions.<sup>(1)</sup> They are the result of the progressive miniaturization of micro-electromechanical systems (MEMS) motivated by the growing demand for high-performance devices with smaller size, higher sensitivity, faster response, higher integration, and lower energy consumption.<sup>(2)</sup> Since the dimensions of devices are scaled down, new materials, technologies, and approaches have been required.

In a simplified way, NEMS can be defined as the scaled-down version of MEMS. Both device structures are similar; they are composed of mechanical moving parts and electronic circuitry. Thus, a device is defined as NEMS if its mechanical structures, generally cantilevers or doubly clamped beams, have at least two dimensions less than 100 nm as in Table 1.

---

\*Corresponding author: [fraga.mariana80@yahoo.com.br](mailto:fraga.mariana80@yahoo.com.br)  
<http://dx.doi.org/10.18494/SAM.2017.1366>

Table 1  
General comparison of MEMS and NEMS technologies.

	MEMS	NEMS
Physics (fundamental theories)	*Classical mechanics *Electromechanics	*Classical and quantum theory *Nano-electromechanics
Manufacturing	Top-down approach	Top-down and bottom-up approaches
Characteristics	Mechanical structures with dimensions on the order of micrometers	*Mechanical structures with at least two dimensions less than 100 nm *High surface-to-volume ratio

A wide comparison between NEMS and MEMS devices shows that NEMS is not a duplication of MEMS in a smaller size. NEMS devices exhibit unique characteristics based on nanoscale effects. Therefore, they have required the development of new simulation and modeling tools. Owing to the size effects, some design parameters negligible in MEMS must be applied to NEMS sensing to achieve a device with high performance.<sup>(3)</sup>

NEMS device characteristics not only depend on the intrinsic properties of the active materials used but are also correlated with the method of device fabrication. Not all materials and processes can be scaled from MEMS to NEMS.<sup>(4)</sup> Regarding the device fabrication, MEMS are manufactured by conventional microelectronics processes combined with micromachining technology. These traditional processing technologies face some fundamental physical limits for NEMS device fabrication. For this reason, there is a continuous development of alternative NEMS fabrication processes. Nowadays, NEMS are built mainly by the top-down and bottom-up fabrication approaches.<sup>(5)</sup> Table 1 compares the basics of NEMS and MEMS technologies.

In terms of material technology, Si has been widely used to build the NEMS devices due to be the main material for IC and MEMS technologies. The advantages of Si include commercial availability of high-quality low-cost wafers, ease of processing into a variety of shapes (membranes, cantilevers, strings, and nanowires) and well-established device processing techniques. However, the Si-based NEMS device has exhibited some drawbacks, for example, the presence of a ~1–2 nm native oxide layer on its surface affects the quality factor of the device. In addition, it has been observed that limitations in strength and flexibility have compromised the performance of Si-based NEMS actuators.<sup>(6)</sup>

The choice of NEMS building materials other than Si has been limited by three main factors: reproducibility, integration with semiconductor technology, and cost. One-dimensional (1D) carbon materials have been shown to be attractive candidates because of their exceptional electrical and mechanical properties associated with their high surface-to-volume ratio, which promises the possibility of high-performance NEMS devices. Carbon nanotubes (CNTs) have established themselves as the main 1D carbon nanostructures for NEMS applications. The main issues for the integration of CNTs with semiconductor technology are summarized in Fig. 1. They can be divided into five major groups:

- (1) Material compatibility: High-temperature growth of 1D carbon (typically 700–1000 °C) can be detrimental to an underlying semiconductor structure; direct growth of the nanostructures into batch-fabricated microsystems is a challenge. The choice of the substrate is also an important issue. Si and Si dioxide are the most common substrates because they are widely used in semiconductor technology.
- (2) Electrical contacts: A range of different metals have been tested for the integration of 1D carbon nanostructures with Si. It has been observed that CNT-Si and CNT-metals have high resistance.

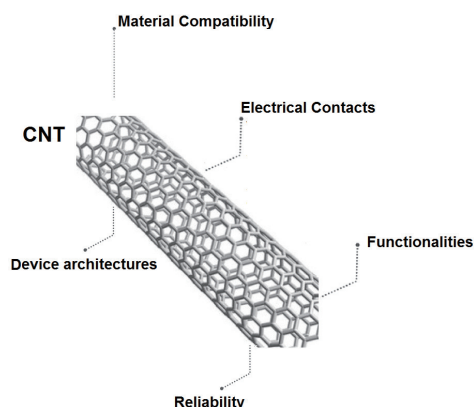


Fig. 1. Issues related to the integration of CNT with semiconductor technology.

- (3) Functionalities: It has been demonstrated that 1D carbon nanostructures add new functionality or improved performance to integrated devices. These nanostructures exhibit great potential as the active material for different sensing applications.
- (4) Device architectures: Connecting several 1D nanostructures into functional devices is a challenge. It is difficult to place each 1D nanostructure at the desired locations with high yield. Another challenge is the distribution of 1D nanostructures with different electrical properties.
- (5) Reliability: For commercial applications, the expected lifetime of the devices must at least be on the order of years. In general, CNTs are durable at high temperatures and in various chemical environments. Failures are associated with the degradation of the interfaces between CNTs and the substrate. The lack of uniformity of the nanostructures also directly affects the device performance.

As can be noted, there are advances still needed for CNTs to achieve large-scale CNT device fabrication and commercialization.<sup>(7)</sup>

A variety of different electromechanical sensor prototypes using CNTs have been reported, particularly those based on piezoresistive strain gauges or field emission.<sup>(8)</sup> CNTs are often used as a beam in NEMS. The mass sensitivities of CNT and Si nanowire beams are compared in Table 2. In this application, the sensitivity is the parameter that indicates the amount of mass necessary to shift the resonant frequency 1 Hz, i.e., the lower the sensitivity, the better the sensor performance. As can be observed, the sensitivity of the CNT beam is less than half that of the Si beam.

Promising results have also been reported for carbon nanowires (CNWs) and nanofibers (CNFs). For example, resonant NEMS based on vertically oriented CNFs have shown potential use in harsh environment sensing and communication devices.<sup>(10)</sup> The main advantage of the use of CNWs in NEMS is that their electronic properties can be well controlled during synthesis. This has not been achieved yet for CNTs. On the other hand, CNWs exhibit a lower degree of flexibility than CNTs, which can limit device fabrication and reliability.<sup>(11)</sup>

Despite advances in growth, characterization, manipulation, and assembly, there are still open issues related to the synthesis and processing of 1D carbon nanostructures for the large-scale production of NEMS. In this context, this review begins by summarizing the synthesis methods and fundamental properties of 1D carbon nanostructures including nanotubes, nanofibers, and nanowires. Next, an overview of the main 1D carbon-based sensors will be introduced. At the same time, the issues involving the sensor fabrication processes will be addressed.

Table 2

Physical properties and mass sensitivity of clamped-clamped beams of Si nanowires and CNTs of equal dimensions (adapted from Ref. 9).

	Young's modulus (GPa)	Mass density (kg/m <sup>3</sup> )	Sm (g/Hz)
Si nanowires	160	2230	$2.92 \times 10^{-23}$
CNTs	1000	2200	$1.14 \times 10^{-23}$

## 2. Fundamental Properties and Synthesis of 1D Carbon Nanostructures

### 2.1 CNTs

The current research on 1D systems has been largely dominated by CNTs, which are formed from graphite sheets in the form of cylinders. They are allotropes of carbon with a nanostructure that can have a length-to-diameter ratio greater than  $10^6$ .<sup>(12)</sup> Figure 2 shows the diameters of CNTs, CNF, and conventional fibers.

CNTs are tubular in shape as can be seen in Fig. 2. A CNT can be defined as a hexagonal arrangement of carbon atoms arranged in a sheet that has been rolled up to form a tube. The tubes contain at least two layers, often many more, and range in outer diameter from about 3 to 30 nm.<sup>(12)</sup> Their extremities are naturally closed by half of a fullerene molecule. CNTs are unique structures with remarkable mechanical and electronic properties, such as the most rigid molecules and flexible and resistant strains ever produced. Mechanically speaking, CNTs have a high Young's modulus (around 1 TPa) and are potentially 30 to 100 times stronger than steel.<sup>(12-17)</sup> Besides, they are the best in conducting both heat and electricity.<sup>(12-17)</sup> Table 3 summarizes some of these properties.

In terms of structure, CNTs may be classified as single-walled (SW) or multiwalled (MW). Selected characteristics of SWCNTs and MWCNTs are shown in Fig. 3. MWCNTs consist of multiple concentric layers of graphene or a stack of graphene sheets rolled up into concentric cylinders. They are larger and consist of many SWCNTs stacked one inside the other. Each nanotube is a single molecule composed of millions of atoms and the length of this molecule can be more than 10  $\mu\text{m}$  long with diameters as small as 0.7 nm.<sup>(18)</sup>

Two different models are proposed to describe the structures of MWCNTs (Fig. 4): (i) Russian doll model where sheets of graphene are arranged into concentric cylinders and (ii) Parchment model where a single graphene sheet is rolled around itself, like a scroll of parchment.<sup>(14)</sup> Like in graphite, the interlayer distance is approximately 3.4 Å.<sup>(14)</sup> The bonding within the CNT walls is covalent, while van der Waals bonding occurs between CNTs, either in a bundle or between CNTs arranged in a MWCNT structure.<sup>(15)</sup>

The SWCNTs are generally narrower than the MWCNTs, with diameters typically in the range of 1–2 nm, and tend to be curved rather than straight.<sup>(12)</sup> Usually, they contain only 10 atoms around the circumference and the thickness of the tube is only one atom thick.<sup>(15)</sup> The structure of a SWCNT can be conceptualized by wrapping a one-atom-thick layer of graphene into a seamless cylinder.<sup>(14)</sup> The way graphene is wrapped is represented by a pair of integers ( $n$ ,  $m$ ). These integers, called Hamada's indices, are coordinates of the point that overlaps after wrapping where the origin is in the honeycomb crystal lattice of graphene.<sup>(14,19)</sup> For the case where  $n = m$ , the CNTs are called achiral armchairs. In the armchair structure, two C–C bonds on opposite sides of

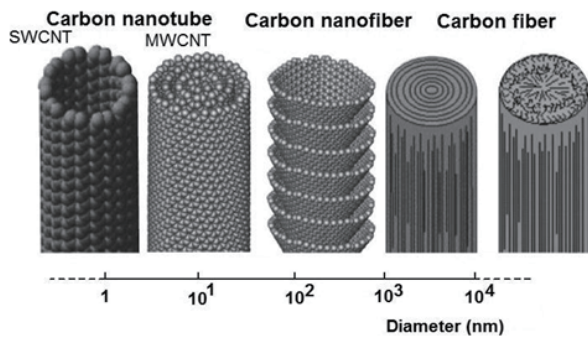


Fig. 2. Schematic of the diameter dimensions on a log scale for some types of carbon structures (adapted from Ref. 13).

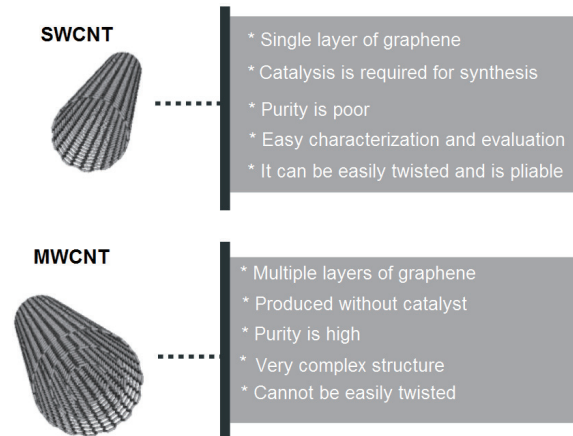


Fig. 3. Some characteristics of SWCNTs and MWCNTs.

Table 3  
Some outstanding properties of CNTs.

Property	Description
Strength	Greater than at least 30 times the strength of steel
Thermal conductivity	More than twice that of diamond
Density	About half that of aluminum
Thermal stability	Stable to 2700 °C
Chemical reactivity	Similar to graphite
Chirality	Metallic or semiconducting

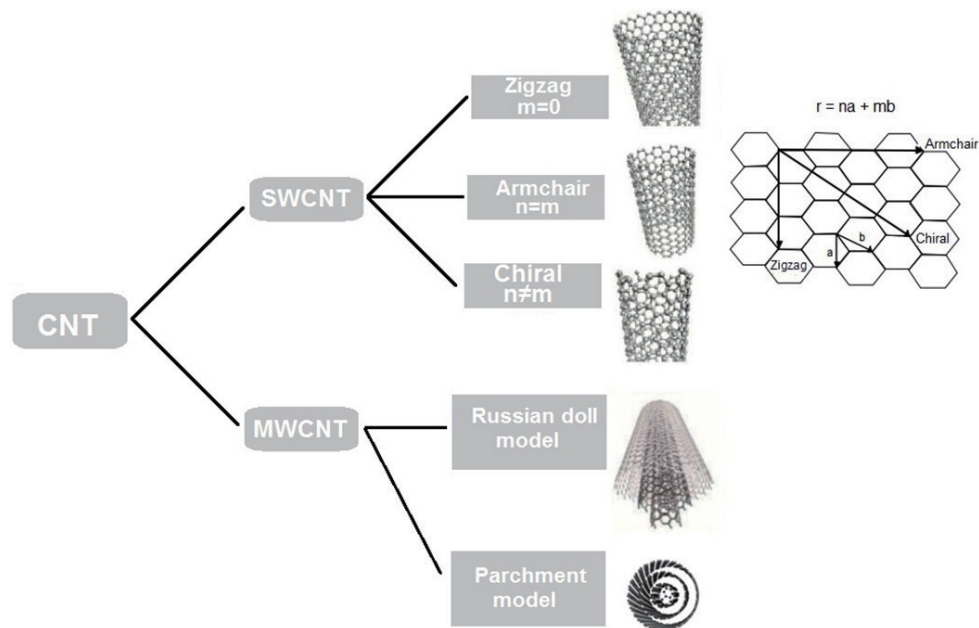


Fig. 4. Classification of CNTs.

each hexagon are perpendicular to the tube axis.<sup>(16)</sup> For the case where  $n \neq 0$  and  $m = 0$ , the CNTs are called achiral zigzags. In the zigzag structure, two C–C bonds are parallel to the tube axis. Otherwise, they are called chiral.<sup>(20)</sup> All other conformations in which the C–C bonds lie at an angle to the tube axis are known as chiral or helical structures.<sup>(16)</sup>

The structural orientation of the CNTs affects the position of the valence and conduction bands. As a result, the CNTs may exhibit metallic or semiconducting behavior. The first type consists of metallic CNTs, where  $n = m$ . CNTs are semiconducting with narrow band gaps when the values of  $m$  and  $n$  are multiples of three. For other cases, CNTs are semiconducting with moderate band gaps.<sup>(19)</sup> Therefore, armchair CNTs are metallic and CNTs with the configurations (6, 3) and (9, 1) are semiconductors; hence, the band gap is tunable by choosing the appropriate CNT structure or Hamada's indices ( $m, n$ ).<sup>(19)</sup>

In theory, metallic CNTs have a carrier mobility of approximately  $10000 \text{ cm}^2/(\text{V}\cdot\text{s})$ , which is better than that of Si. They can carry an electrical current density of approximately  $4 \times 10^9 \text{ A/cm}^2$ , which is three orders of magnitude higher than that of a typical metal such as copper that has interconnect current densities limited by electromigration.<sup>(21)</sup>

It is also valuable to note that the rules for metallic and semiconducting CNTs here discussed have some exceptions. Curvature effects in small-diameter CNTs can affect the electrical properties. In this case, for example, a CNT with Hamada's indices of (5, 0) according to the rule should be semiconducting, but is metallic,<sup>(20)</sup> while some small-diameter tubes expected to be metallic have a small gap in the band structure.<sup>(19)</sup> Armchair CNTs remain unchanged.

In the same way as the band gap structure, the chirality and the tube diameter are other important parameters that affect the properties of CNTs. For example, they have strong dependence on the binding energy, size, and bright-dark splitting of excitons in semiconducting CNTs.<sup>(22)</sup> Furthermore, it has been reported that they simultaneously affect the solubility of SWCNTs.<sup>(23)</sup> The chirality and the tube diameter are established during CNT synthesis and may be modified subsequently by treatment and purification processes.

Chirality is given for the chiral angle of CNTs, which is the angle between the C–C bonds and the tube axis. Both the chirality ( $\theta$ ) and diameter ( $d$ ) of an ideal CNT can be calculated from Hamada's indices ( $n, m$ ) as follows:

$$d = \frac{a}{\pi} \sqrt{n^2 + nm + m^2}, \quad (1)$$

$$\theta = \arctan\left(\frac{m\sqrt{3}}{2n + m}\right), \quad (2)$$

where  $a$  is the length of the unit vectors in the 2D lattice of graphene ( $a = 0.246 \text{ nm}$ ).<sup>(12)</sup>

The synthesis of CNTs (single or multiwalled) can be performed by different methods, mainly gas phase processes. All these methods have three ingredients in common: (i) carbon source, (ii) catalyst nanoparticle species, and (iii) energy input.<sup>(14)</sup> These ingredients may provide various ways of synthesis. When the carbon source is provided in liquid or gaseous form, the generic term of "medium- or low-temperature method" is used.<sup>(14)</sup> Therefore, the term "high-temperature method" is used to define processes that involve the sublimation of the solid source (graphite) at temperatures greater than  $3200 \text{ }^\circ\text{C}$ .<sup>(14)</sup> The first CNTs were synthesized by this technique.

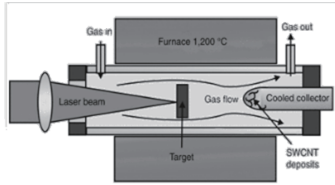
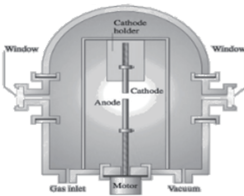
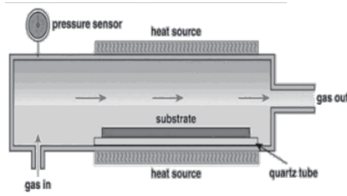


The catalyst species necessary for CNT synthesis is typically transition-metal nanoparticles (diameter less than 10 nm) formed on a support substrate. For this purpose, iron, cobalt, and nickel are the most effective transition metals used. Metal catalyst nanoparticles are crucial in CNT growth. At high temperature, these metals have high solubility of carbon and a high diffusion rate, which is very helpful during the CNT growth process.<sup>(24)</sup> Furthermore, the melting point for such catalyst candidates is suitable for synthesizing CNTs since the growth temperature is in the range of 700–900 °C.<sup>(25)</sup> There are other metals in the same group with potential for CNT growth, such as chrome and copper and their alloys and compounds. Moreover, different deposition methods of metal catalyst nanoparticles have been investigated. These methods are well reported in a review published by Azam *et al.*<sup>(24)</sup>

Currently, laser ablation, electric arc discharge, and chemical vapor deposition (CVD) are the most common and well-explored techniques of synthesizing CNTs. A comparison of them is shown in Table 4. The CVD technique is the most reported in the literature owing to advantages such as lower processing temperature, possibility of controlling the CNT structure, high purity as well as large-quantity production.<sup>(26,27)</sup>

In the electric arc discharge method, a high-current electric arc goes through graphite electrodes in the presence of catalytic particles forming CNTs and soot.<sup>(15,28)</sup> This process is performed in a chamber filled with argon or helium gas.<sup>(14)</sup> The plasma generated in the chamber presents an extremely high temperature that can reach 600 °C.<sup>(15)</sup> The carbon atoms generated by graphite sublimation migrate towards colder zones within the chamber, resulting in CNT accumulation on the cathode. Evidently, electric arc discharge is considered a high-temperature method for CNT deposition. This technique was first reported by Iijima for producing microtubules of graphitic carbon.<sup>(29)</sup> The electric arc discharge method presents a yield of 30 wt.% and can produce both SWCNTs and MWCNTs with few or no structural defects.<sup>(17)</sup> The presence of specific metal catalytic particles determines the production of MWCNTs or SWCNTs.<sup>(15)</sup> However, for an anode

Table 4  
Comparison of CNT production techniques.

	Laser ablation	Arc discharge	CVD
Typical reactor			
Process control	Difficult	Difficult	Easy, can be automated
Production rate	Low	Low	High
Energy requirement	High	High	Moderate
Product purity	High	High	High
Cost	High	High	Low

of pure graphite, the products are fullerenes, amorphous carbon, and some graphitic sheets, but no nanotubes.<sup>(15)</sup> For an anode of graphite and metal, the tubes tend to be short (50  $\mu\text{m}$  or less) and deposited in random sizes and directions.<sup>(17)</sup>

Like electric arc discharge, laser ablation is also considered a high-temperature technique for CNT deposition because it involves the sublimation of graphite. In laser ablation, a pulsed laser (Nd, Nd:YAG, or  $\text{CO}_2$ ) is irradiated onto the surface of a graphite target in the presence of metal catalyst. The laser vaporizes graphite by scanning its surface at higher temperatures, around 1000–1200  $^\circ\text{C}$ .<sup>(14,24)</sup> The fullerenes and CNTs produced by the sublimation of graphite are displaced by an inert gas flow (helium or argon), coalesce in the gas phase, and finally are deposited on a cooled copper collector.<sup>(14)</sup> Using laser ablation, it is possible to define the SWCNT or MWCNT structure by specifying the metal catalytic particles. This was the first method used to produce  $\text{C}_{60}$ : Buckminsterfullerene reported in the literature.<sup>(30)</sup> In addition, laser ablation can produce primarily SWCNTs with up to 70 wt.%, and with a diameter range that can be controlled by varying the reaction temperature.<sup>(17)</sup> However, laser ablation requires very expensive lasers, making it by far the most costly method.<sup>(17)</sup> The advantage of laser ablation is that it lends itself well to the implementation of diagnostics and *in situ* observations during the CNT growth.<sup>(14)</sup>

In CVD, CNTs are produced by thermal decomposition of precursor gases, such as methane, ethylene, toluene, xylene, camphor, acetylene, and benzene.<sup>(15)</sup> These precursors are the carbon source for the CNT synthesis. As the sources are provided in gaseous form, the generic term of the low-temperature method is used for CVD. CNT synthesis by CVD occurs at temperatures between 500–1000  $^\circ\text{C}$ . The CVD method is catalytically driven: a transition-metal catalyst is used in conjunction with the thermal decomposition of a hydrocarbon vapor to produce nanotubes.<sup>(15)</sup> CVD produces CNTs with 20 to 100 wt.%. Among the three methods described, it is the easiest to scale up to industrial production and may possibly yield nanotubes of great length.<sup>(17)</sup> Moreover, it has the best cost/benefit ratio for the production of CNTs. However, CNTs made by CVD are usually multiwalled and are often riddled with defects. As a result, the tubes have only one-tenth the tensile strength of those made by electric arc discharge.<sup>(17)</sup> High-quality nanostructures are often required for NEMS device applications. Despite the issue of quality, CVD-based methods have been employed in the development of 1D carbon devices, because they allow the CNT growth directly on the substrate surface, enabling the integration for device applications. On the other hand, although CVD processes use lower temperatures than other CNT synthesis methods, the temperatures involved (greater than 500  $^\circ\text{C}$ ) are not compatible with some substrate materials and microelectronics/microfabrication processes. Hence, there is much interest in CNT growth by low-temperature techniques.

Plasma-enhanced CVD (PECVD) has often been reported as the most versatile technique for CNT deposition.<sup>(31–36)</sup> It is especially attractive because it enables CNT deposition on temperature-sensitive substrates and exhibits compatibility with device fabrication processes.<sup>(14)</sup> Furthermore, owing to the high deposition rate of PECVD, the structures can be formed in a short time, which is of interest from the industrial viewpoint.<sup>(32)</sup>

Some studies have revealed that PECVD is able to grow CNTs at 120  $^\circ\text{C}$  using nickel as a catalyst in a  $\text{C}_2\text{H}_2/\text{NH}_3$  system<sup>(33)</sup> and nickel and copper as catalysts in a  $\text{C}_2\text{H}_2/\text{Ar}$  system.<sup>(32)</sup> The low-temperature processing is possible since high-energy electrons (3–4 eV) supply the energy needed for chemical reactions in the gas or plasma phase while the gas itself is relatively cool (27–227  $^\circ\text{C}$ ).<sup>(34)</sup> More recently, PECVD has been investigated for its ability to produce vertically aligned nanotubes.<sup>(23)</sup> For this, a variety of different plasma sources have been investigated.<sup>(34–36)</sup>



For the production of vertically aligned CNTs, dielectrophoresis is a simple but versatile method that has proven to be effective in aligning CNTs at small and large scales.<sup>(37)</sup> Figure 5(a) illustrates the configuration of the experimental system for dielectrophoresis of the CNTs. This is basically composed of an alternating current (AC) source and micromachined electrodes (for example, in the form of “teeth”) on the substrate. The AC source is connected to the electrodes through two metal probes. After the instruments are set up, a droplet of the CNT solution is placed in the area between the electrodes using a syringe and the AC signal source is switched on, promoting the generation of an electric field between the electrodes. The electric field exerts dielectrophoretic forces on the CNTs and forces them to rotate along the field lines [Fig. 5(b)]. The CNTs can be deposited on the substrate with this orientation. After a short period (~30 s) of dielectrophoresis, the AC signal is switched off and the CNT solution is removed with another syringe.<sup>(38)</sup> This method can be carried out at room temperature with low voltages.

In the field of CNT research, dielectrophoresis was first introduced as a method of assembling and contacting individual or bundled SWCNTs on predefined electrode structures.<sup>(39)</sup> It was then demonstrated that dielectrophoresis allows for an electronic type-specific sorting of SWNTs on the basis of the difference in the polarizability of semiconducting and metallic nanotubes.<sup>(40)</sup> Additionally, dielectrophoresis can be easily incorporated into device fabrication<sup>(41)</sup> and eventually used in wafer-level-controlled deposition.<sup>(42)</sup>

In accordance with the method and the synthesis parameters used, different types of CNTs can be produced. Chirality, number of walls, structural defects, tube diameter, and length are important characteristics that directly affect CNT properties. Such characteristics can be obtained by various material characterization techniques. For example, Raman spectroscopy can be used to investigate the structural defects and predict the tube diameter;<sup>(43)</sup> transmission electron microscopy (TEM) is particularly useful for determining the chirality,<sup>(44)</sup> the length,<sup>(45)</sup> and the number of walls. The choice of ideal properties is essential for each specific application.

Since the discovery of CNTs, numerous applications have been proposed. SWCNTs have been shown to be strong candidates for sensing-element applications. Semiconducting CNTs change their electrical resistance dramatically when exposed to halogens, alkalis, and other gases at room temperature, raising hopes for realizing better chemical sensors.<sup>(17)</sup> From the commercial viewpoint, applications in semiconducting gas sensors, DNA sensors, infrared sensors, and electron field emitters of displays<sup>(46)</sup> appear to have defined market niches and are technologically mature.<sup>(47)</sup>

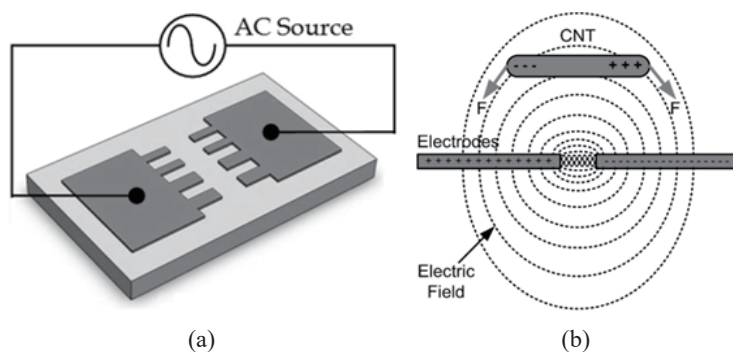


Fig. 5. (a) Experimental system for the dielectrophoresis of CNTs and (b) principle of dielectrophoresis deposition and alignment of CNT (adapted from Ref. 38).

## 2.2 CNFs

CNFs are cylindrical nanostructures with graphene layers arranged as stacked cones, cups, or plates. They have high aspect ratios ( $>100$ ) with diameters greater than 100 nm and lengths exceeding 30  $\mu\text{m}$ . The size of CNFs places them between CNTs and commercially available carbon fibers (CFs) as shown in Fig. 2.<sup>(48,49)</sup> When the CNFs are compared with conventional CFs, the first difference is that CFs have micrometer-order diameters. Besides the diameter, the structures of the CNFs are different from those of conventional CFs. In a CF, the carbon atoms are bonded together as crystals that are more or less aligned parallel to the long axis of the fiber and the crystal alignment gives the fiber a high strength-to-volume ratio.<sup>(50)</sup> In addition, CNFs are different from CNTs. Their geometry is different from that of concentric CNTs containing an entire hollow core, because they can be visualized as regularly stacked truncated conical or planar layers along the filament length.<sup>(50)</sup> Such unique structure leads to semiconducting behavior and with chemically active end planes on both the inner and outer surfaces of the nanofibers, thereby making them useful as supporting materials for catalysts, reinforcing fillers in polymeric composites, hybrid-type filler in carbon-fiber-reinforced plastics, and photocurrent generators in photochemical cells.<sup>(48)</sup> For sensing purposes, this 1D carbon-based material has been successfully applied as a sensor for toxic and nontoxic gases,<sup>(51–53)</sup> a strain sensor,<sup>(54,55)</sup> an electromagnetic interference shield, and a thermal interface.<sup>(56)</sup>

Unlike the conventional CF, the CNF can be prepared mainly by two techniques: catalytic thermal CVD and electrospinning. By catalytic thermal CVD, two types of CNF can be prepared, namely, the cup-stacked CNF and the platelet CNF.<sup>(50,57,58)</sup> Briefly, CNFs are produced by the catalytic CVD of a hydrocarbon (such as natural gas, propane, acetylene, benzene, ethylene, etc.) or carbon monoxide over the surface of a metal (Fe, Ni, Au, Co) or metal alloy (such as Ni–Cu, Fe–Ni) catalyst.<sup>(59–61)</sup> The catalyst can be deposited on a substrate or directly fed with the gas phase.<sup>(62)</sup> The reaction is usually carried out in a reactor operated at a temperature of 500–1500  $^{\circ}\text{C}$ .<sup>(63)</sup> The hydrocarbon decomposes on the metal catalyst; this decomposition both nucleates and causes the CNFs to grow.<sup>(64)</sup> Generally, the structures of the CNF are governed by the shapes of the catalytic nanosized metal particles.<sup>(63)</sup> The growth mechanism has been proven to be the deposition of the hydrocarbons dissolved in the metal particle on the metal surface as graphitic carbon.<sup>(48)</sup> Readers interested in the growth of CNFs by catalytic thermal CVD are advised to refer to a general review by Al-Saleh and Sundararaj.<sup>(65)</sup>

Electrospinning is another widely used method of producing CNFs. Recently, Inagaki *et al.* published a review on CNFs produced by electrospinning and carbonization, summarizing the method in accordance with their structure and properties.<sup>(66)</sup> More recently, Zhang *et al.* reviewed the advances in the preparation and applications of CNFs prepared by electrospinning.<sup>(67)</sup>

In the electrospinning method, polymeric nanofibers must be used as the precursors of the CNFs. Hence, the final properties of the CNFs are dependent on the types of polymer solution and polymer nanofiber processing parameters. Polyacrylonitrile (PAN) and pitch are the most frequently used polymers. In addition, poly(vinyl alcohol) (PVA), polyimides (PIs), polybenzimidazole (PBI), poly(vinylidene fluoride) (PVDF), phenolic resin, and lignin were also used.<sup>(66)</sup> A conventional electrospinning setup involves three major components: a high-voltage power supply, a spinneret (e.g., a syringe or pipette tip), and a grounded collector (typically a flat metal plate or a rotating drum).<sup>(68)</sup> In short, the electrospinning technique is based on the application of an electric field to a drop of polymer solution at the tip of a spinneret. As the intensity of the electric field increases, the surface

of this drop elongates to form a conical shape known as the Taylor cone.<sup>(69)</sup> When the applied electric field reaches a critical value, the repulsive electrical forces overcome the surface tension of the drop, and a charged jet of the solution is ejected from the tip of the cone and accelerates downfield. An electrohydrodynamic whipping instability of the jet occurs between the tip and the collector, which leads to further stretching of the liquid filament and the evaporation of the solvent to generate solidified continuous, micro- or nanofibers on the grounded collector.<sup>(70)</sup> Once the polymer nanofibers have been successfully prepared, a heat treatment (up to 1000 °C in a specific environment) will be applied to carbonize the polymer nanofibers to form CNFs. Generally, volume and weight changes will occur during the carbonization process, resulting in a decrease in the diameter of the CNFs. The morphology, purity, crystallinity, diameters, and porosity are governed by the parameters of the heat treatment process, such as atmosphere and temperature.<sup>(70,71)</sup>

The dimension and the structural, electrical, mechanical, and thermal properties of the CNFs depend on the production technique and post-treatment methods.<sup>(72)</sup> Table 5 summarizes some typical properties of vapor-grown CNFs (VGCNFs), electrospun CNFs, CFs, SWNTs, and MWNTs.

Comparing the properties shown in Table 5, we can see that CNFs have worse mechanical and electrical properties than CNTs. CNFs also have larger diameters, higher density, and lower aspect ratios than those of CNTs. However, because of their availability and relatively low price, CNFs are an excellent alternative to CNTs. In addition, CNFs could be used for research purposes to accumulate knowledge that might be transferable to the more expensive CNTs. MWCNTs are 2–3 times more expensive than VGCNFs, and SWCNTs are even more expensive. In 2009, the prices of VGCNFs, MWCNTs, and 90% pure SWCNTs were \$200/kg, \$450/kg, and \$50000/kg, respectively.<sup>(73)</sup> A comparison of the qualities of CNFs produced by the three major techniques, namely, CVD, traditional spinning, and electrospinning, in terms of diameter, electrical conductivity, and cost has been presented by Zhang *et al.*<sup>(75)</sup> It was shown that electrospinning is much more effective for producing CNFs with small diameters and high electrical conductivities than the traditional spinning technique. The cost of electrospun CNFs is expected to be much lower than that of CNFs produced by CVD methods because of the simpler processes.

Table 5  
Typical properties of VGCNF, electrospun CNFs, CFs, SWNTs, and MWNTs.<sup>(65,66,73–75)</sup>

Property	VGCNF	Electrospun CNF	CF	SWCNT	MWCNT
Diameter (nm)	50–200	50–250	7300	0.6–1.8	5–50
Length (μm)	50–100	—	3200	—	1–50
Aspect ratio	250–2000	—	440	100–10000	100–10000
Specific surface area (m <sup>2</sup> /g)	150–200	20–2500	—	—	1000–1350
Density (g/cm <sup>3</sup> )	2	1.5–2.0	1.74	~1.3	~1.75
Thermal conductivity (W/m·K)	1950	5–1600	20	3000–6000	3000–6000
Electrical resistivity (Ω·cm)	1 × 10 <sup>-4</sup>	—	1.7 × 10 <sup>-3</sup>	1 × 10 <sup>-3</sup> –1 × 10 <sup>-4</sup>	2 × 10 <sup>-3</sup> –1 × 10 <sup>-4</sup>
Tensile strength (GPa)	2.92	—	3.8	50–500	10–60
Tensile modulus (GPa)	240	50–250	227	1500	1000

For electrical applications, CNFs are also competitive with CFs, owing to the lower loading of VGCNFs than that of CFs required to achieve certain electrical conductivities. The volume resistivity of normal VGCFs after graphitization is  $6 \times 10^5 \Omega \text{ cm}$ .<sup>(65,73)</sup> The thermal conductivity of 1950 W/(m K) of VGCNFs is the highest among all commercial CFs.<sup>(65)</sup> The thermal conductivity of MWNTs experimentally measured is around 3000 W/(m K).<sup>(65,76)</sup> This value is much lower than the 6600 W/(m K) theoretically estimated for SWNTs using molecular dynamics simulations.<sup>(76)</sup>

### 2.3 CNWs

Nanowires can be defined as structures that have a lateral size limited to less than 10 nm and an unconstrained longitudinal size. At these scales, quantum mechanical effects are important, which led to the term “quantum wires”. There are many different types of nanowires, including metallic (e.g., Ni, Pt, Au), semiconducting (e.g., Si, GaN, etc.), and insulating (e.g., SiO<sub>2</sub>, TiO<sub>2</sub>).<sup>(77,78)</sup> Among them, there is the class of CNWs. CNWs are novel nanostructures of ever-increasing importance in nanoscience and nanotechnology. Their potential use in NEMS and nanoelectronics may be considerably facilitated by their far more flexible technology (compared with CNTs), controllability of their positioning, and reproducibility of their electrical and structural parameters.

CNWs are composed of both sp<sup>2</sup> and sp bonds. The known carbon allotropes are usually based on one of the three types of bonding: sp<sup>3</sup> (diamond), sp<sup>2</sup> (graphite, fullerenes, and nanotubes), and sp (C chain and carbyne). By high-resolution transmission electron microscopy (HRTEM) and Raman spectroscopy, Zhao *et al.* confirmed that a CNW consists of a MWCNT (sp<sup>2</sup>) with a 1D linear C chain (sp) inserted into its innermost tube of 0.7 nm diameter.<sup>(79)</sup> When a CNW is modeled using a SWCNT with a linear C chain inside its hollow core, first-principles calculations show that the C–C bond length in a C chain is tuned by the projected C–C distance of SWNT on the nanotube axis.<sup>(79)</sup>

Relatively few methods have been developed for the fabrication of CNWs. The most common are based on the CNT growth methods discussed in Sect. 2.1. De Volder *et al.*, using standard lithography, oxygen plasma treatment, and thermal processing, fabricated and integrated vertically aligned forests of amorphous CNWs.<sup>(80)</sup> Amma *et al.* synthesized CNWs by the pyrolysis of polymer precursors in the pores of alumina membranes and aligned the CNWs using electrostatic interactions with monolayers at the bottom of the lithographically formed wells.<sup>(81)</sup> A more complex technique of producing CNWs is focused ion beam (FIB) writing.<sup>(82)</sup> The idea to make CNWs on diamond surfaces by FIB writing resulted from the search of a technology capable of the reproducible fabrication of carbon electronic nanostructures. Since the current technology of individual CNTs has not met the challenge of reproducible manipulation, positioning, and patterning, alternative ways must be found. The FIB-written CNWs could be one approach, which, to some extent, could circumvent this problem. The work of Zaitsev *et al.* showed that FIB irradiation could be used to purposely form CNWs and nanodots of a predetermined geometry in predetermined configurations on a diamond substrate.<sup>(82,83)</sup> It was noted that the same FIB irradiation can be simultaneously used to make interconnections between the nanowire-nanodot structures, as well as to fabricate terminal contact pads to connect the nanostructures to the outside world. Moreover, it was found that the CNW structures were temperature sensitive and could be used as temperature nanosensors.<sup>(82)</sup> A novel property of the FIB-written carbon nanostructures has recently been discovered: their chemical sensitivity.<sup>(84)</sup>

### 3. Applications of 1D Carbon Nanostructures as Sensing Elements

Small sensors with simple construction for large-scale production, high sensitivity, convenient operation, and fast and stable response are desirable to meet the demands of different applications.<sup>(67)</sup> Several types of nanosensors based on 1D carbon nanostructures (nanotubes, nanofibers, or nanowires) can be developed. In general, the proposed sensors are categorized into two main groups: (i) those that interact with structures and surfaces on atomic and molecular levels (e.g., CNTs used as AFM probe tips) and (ii) those that interact with the macroscopic environment (e.g., CNT beam-based sensor).<sup>(1)</sup>

The manufacturing of sensors using 1D carbon nanostructures involves the integration of semiconductor and carbon technologies. For most of these sensors, Si is the semiconductor material chosen as substrate. This necessitates that 1D carbon growth be compatible with Si device processes. Conventional CVD CNT growth and device fabrication techniques are unable to fully meet this requirement owing to a lack of precise control over nanotube positioning and orientation.<sup>(85)</sup> Some methods have been developed to enable the manufacture of NEMS based on 1D carbon nanostructures. These methods are divided in two groups: (i) direct 1D carbon nanostructure growth and integration (also called *in situ* growth techniques), which is characterized by the control of the position of the nanostructures on the substrate, and (ii) 1D carbon nanostructure assembly and integration (also called postgrowth manipulation), which is characterized by moving the previously synthesized nanostructures to the desired position.<sup>(8,86)</sup>

Prototypes of 1D carbon sensors have been developed on the basis of different transduction principles and with different device architectures. In this review, our focus is on NEMS-based sensors using suspended structures made from CNT (or CNF or CNW). In the next section, examples of these sensors, their fabrication processes and potential applications will be presented.

#### 3.1 Examples of NEMS-based sensors using 1D carbon nanostructures

Chiu *et al.* observed that resonators based on individual double-clamped SWCNTs are capable of atomic-scale mass sensing and determining the inertial mass of atomic species.<sup>(87)</sup> The resonator geometry proposed by them consists of a single-electron transistor, as shown in Fig. 6. This device was manufactured by the following fabrication steps: (i) CNTs are grown from a catalyst island under either pure CH<sub>4</sub> or CH<sub>4</sub>/H<sub>2</sub> mixture on an oxidized Si wafer, (ii) an electron beam is used to attach Pd/Au source/drain electrodes and a side gate, and (iii) SiO<sub>2</sub> was etched using buffered HF to suspend the CNT within the window. The results of the analysis performed on the resonator indicate its potential for ultraminiaturized mass spectroscopy or arrays, which will enable on-chip detection and identification of unknown analytes, as well as the study of single-atom adsorption and desorption.<sup>(87)</sup>

CNTs have also been used as sensors for nanofluidic applications. In Fig. 7, the CNT fluidic sensor recently proposed by Son *et al.* is shown.<sup>(88)</sup> SWCNTs with diameters less than 2.5 nm were synthesized directly on a 220-nm-thick thermal oxide layer on a conducting Si substrate. A conventional process of metal evaporation (Cr/Au) and lift-off was used to define the drain (D) and source (S) electrodes. In order to fabricate the partially suspended device, a trench was chemically etched beneath the SWNT at the center of the structure by HF treatment followed by treatment with a KOH solution. In terms of device performance, the sensitivity of the suspended SWNT devices is more than 10 times greater than that of any nanoscale FET device reported to date. However,



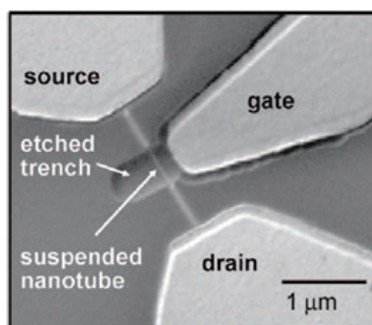


Fig. 6. Doubly clamped suspended CNT nanomechanical resonator.<sup>(87)</sup>

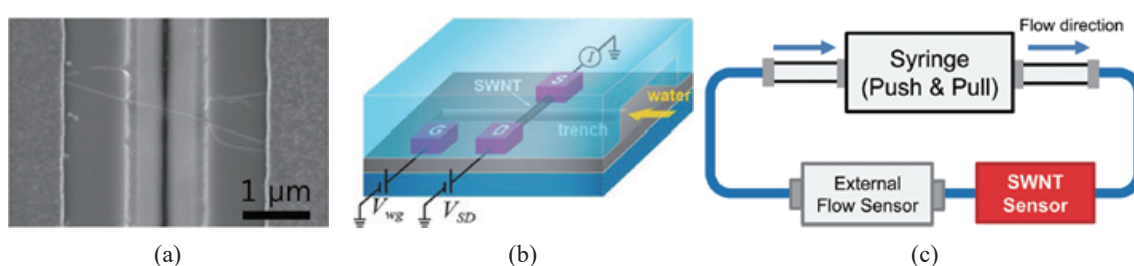


Fig. 7. (Color online) NT fluidic sensor: (a) SEM image of a partially suspended SWCNT device, (b) schematic illustration of the sensor, and (c) schematic of the operation of the sensor.<sup>(88)</sup>

they observed a large sample-to-sample variation in SWNT device performance, influenced by various factors such as nanotube chirality, metal contacts, defects, surface-induced deformation, and chemical environment. In general, the high sensitivity obtained for suspended SWNT devices shows their great potential as biological and chemical detectors.

In NEMS resonator applications, the CNT platform has competed with the Si nanowire. Table 6 shows the sensitivities of state-of-the-art resonant mass sensors based on CNTs and Si nanowires. As explained in the introduction of this review, for resonant structures, the lower the sensitivity, the better the sensor performance. Note that CNTs have the smallest dimensions and better sensitivity than Si nanowire.

Lee *et al.*<sup>(89)</sup> reported a CNF NEMS device prototype operating as nanoscale cantilevers supported at one end (Fig. 8). Nickel deposited by electron-beam evaporation was used as the catalyst for the CNFs. The control size, position, and density of CNFs were determined by high-resolution photolithography to pattern and fabricate large arrays of Ni catalyst dots. The measured multiple-mode resonance response from this single CNF indicates its potential for enabling NEMS that can be employed for resonant sensing and detection of radiation, adsorption, and other physical and/or biochemical processes.

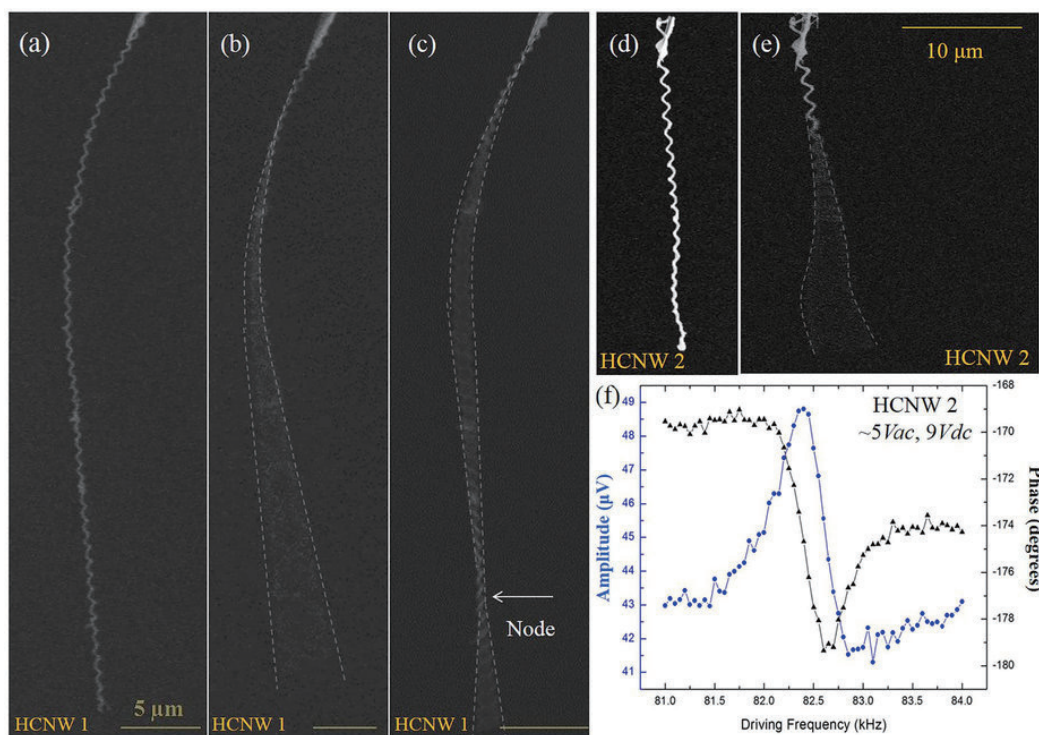
Another device based on CNF was reported by Kaul,<sup>(90)</sup> who performed *in situ* mechanical and electrical measurements by coupling a single CNF with a nanoprobe inside an SEM. A high-amplitude mechanical vibration or resonance was observed. This can enable applications of the CNFs in mass sensing for detecting target species by appropriately functionalizing their surface.



Table 6

Sensitivities of state-of-the-art resonant mass sensors based on CNT and Si nanowires (adapted from Ref. 9).

Material	Dimensions (nm)	Sensitivity (yg/Hz)
CNT	$l = 205, d = 1.78$	0.01
CNT	$l = 900, d = 1.00$	0.09
Si nanowire	$l = 1800, d = 30$	0.06

Fig. 8. (Color online) Resonance frequencies of singly clamped HCNW cantilever.<sup>(92)</sup>

Heo *et al.* employed a single CNW as a hydrogen gas sensor to test the feasibility of the system as an electrochemical sensor platform.<sup>(91)</sup> In this gas sensing system, the suspended CNW was fabricated through conventional simple photolithography and pyrolysis. An advantage of this sensor is that only simple conventional batch microfabrication processes were used. In addition, the functionality of the nanowire systems can allow applications of the single suspended CNW to be extended to the labeling of free biosensors based on AC voltammetry.

The mechanical resonances of a singly clamped helically coiled CNW (HCNW) were investigated by Saini *et al.* by the harmonic detection of resonance (HDR) (Fig. 8).<sup>(92)</sup> Liquid-precursor-based thermal CVD was used to synthesize a forest of randomly oriented HCNWs. For HDR measurements, an isolated HCNW mounted on an electrochemically etched tungsten tip (W-tip) was used as the cantilever. The W-tip was brought into contact with double-sided conducting carbon adhesive tape and then used to isolate a single HCNW from the forest. An interesting result was that these nanowires exhibit modes at much lower driving forces relative to those needed for linear CNT cantilevers.

#### 4. Final Remarks

In this review, we discussed the potential of 1D carbon nanostructures, including nanotubes, nanofibers, and nanowires, for NEMS-based sensors. An overview of the properties and synthesis methods of these nanostructures was introduced. Promising prototypes of 1D carbon-based sensors have been described. We concluded that to enable large-scale production of these sensors, further advances are necessary in the synthesis and integration of 1D carbon nanostructures, especially in relation to control and reproducibility. Besides, although the CNT platform will become more established, CNFs and CNWs are also viable alternatives.

#### Acknowledgements

The authors acknowledge the Brazilian agencies FAPESP (process 14/18139-8) and CNPq (process 160261/2015-5 and 301982/2015-5).

#### References

- 1 C. Hierold: MEMS NEMS Proc. GMe Forum (2005) p. 7.
- 2 M. Li, E. B. Myers, H. X. Tang, S. J. Aldridge, H. C. McCaig, J. J. Whiting, R. J. Simonson, N. S. Lewis, and M. L. Roukes: *Nano Lett.* **10** (2010) 3899.
- 3 K. L. Ekinici and M. L. Roukes: *Rev. Sci. Instrum.* **76** (2005) 061101.
- 4 C. Yang: From MEMS to NEMS: Scaling Cantilever Sensors, Master of Science Thesis, Electrical Engineering, Technische Universiteit Delft (2012).
- 5 B. Bhushan: Springer Handbook of Nanotechnology (Springer, 2010).
- 6 Y. Tao, P. Navaretti, R. Hauert, U. Grob, M. Poggio, and C. L. Degen: *Nanotechnology* **26** (2015) 465501.
- 7 S. Stobbe, P. E. Lindelof, and J. Nygard: *Semicond. Sci. Technol.* **21** (2006) S10.
- 8 C. Hierold, A. Jungen, C. Stampfer, and T. Helbling: *Sens. Actuators, A* **136** (2007) 51.
- 9 J. L. M. Gamarra: NEMS/MEMS Integration in Submicron CMOS Technologies, PhD Thesis, submitted to Universidad Autonoma de Barcelona (2014).
- 10 A. B Kaul, K. G. Megerian, A. T. Jennings, and J. R. Greer: *Nanotechnology* **21** (2010) 315501.
- 11 C. Ke and H. D. Espinosa: Handbook of Theoretical and Computational Nanotechnology, eds. M. Rieth and W. Schommers (American Scientific Publishers, 2005) Vol. 1, pp. 1–38.
- 12 N. Saifuddin, A. Z. Raziah, and A. R. Junizah: *J. Chem.* **2013** (2013) 676815.
- 13 Y. A. Kim, T. Hayashi, M. Endo, and M. S. Dresselhaus: Springer Handbook of Nanomaterials (Springer, 2013).
- 14 C. Journet, M. Picher, and V. Jourdain: *Nanotechnology* **23** (2012) 142001.
- 15 S. B. Sinnott and R. Andrews: *Crit. Rev. Solid State Mater. Sci.* **26** (2001) 145.
- 16 M. Terrones: *Annu. Rev. Mater. Res.* **33** (2003) 419.
- 17 P. G. Collins and P. Avouris: *Sci. Am.* **283** (2000) 62.
- 18 M. Meyyappan, L. Delzeit, A. Cassell, and D. Hash: *Plasma Sources Sci. Technol.* **12** (2003) 205.
- 19 N. Hamada, S. Sawada, and A. Oshiyama: *Phys. Rev. Lett.* **68** (1992) 1579.
- 20 X. Lu and Z. Chen: *Chem. Rev.* **105** (2005) 3643.
- 21 S. Hong and S. Myung: *Nat. Nanotechnol.* **2** (2007) 207.
- 22 R. B. Capaz, C. D. Spataru, S. Ismail-Beigi, and S. G. Louie: *Phys. Rev., B* **74** (2006) 121401.
- 23 K. Lee and C. R. Park: *RSC Adv.* **4** (2014) 33578.
- 24 M. A. Azam, N. N. Zulkapli, Z. M. Nawawi, and N. M. Azren: *J. Sol-Gel Sci. Technol.* **73** (2015) 484.
- 25 Y. Homma, Y. Kobayashi, T. Ogino, D. Takagi, R. Ito, Y. J. Jung, and P. M. Ajayan: *J. Phys. Chem. B* **107** (2003) 12161.
- 26 K. P. Yung, J. Wei, and B. K. Tay: 2004 Electron. Packag. Technol. Conf. (2004) pp. 138–142.
- 27 X. Chen, R. Wang, J. Xu, and D. Yu: *Micron* **35** (2004) 455.
- 28 M. Kundrapu, J. Li, A. Shashurin, and M. Keidar: *J. Phys. D: Appl. Phys.* **45** (2012) 315305.
- 29 S. Iijima: *Nature* **354** (1991) 56.

- 30 H. W. Kroto, J. R. Heath, S. C. O'Brien, R. F. Curl, and R. E. Smalley: *Nature* **318** (1985) 162.
- 31 L. A. Gautier, V. L. Borgne, and M. A. E. Khakani: *Carbon* **98** (2016) 259.
- 32 F. H. O. Carvalho, A. R. Vaz, S. Moshkalev, and R. V. Gelamo: *Mater. Res.* **18** (2015) 860.
- 33 S. Hofmann, C. Ducati, J. Robertson, and B. Kleinsorge: *Appl. Phys. Lett.* **83** (2003) 135.
- 34 M. Meyyappan: *J. Phys. D: Appl. Phys.* **42** (2009) 213001.
- 35 M. Meyyappan, L. Delzeit, A. Cassell, and D. Hash: *Plasma Sources Sci. Technol.* **12** (2003) 205.
- 36 E. C. Neyts: *Front. Chem. Sci. Eng.* **9** (2015) 154.
- 37 P. Li and W. Xue: *Nanoscale Res. Lett.* **5** (2010) 1072.
- 38 W. Xue and P. Li: *Carbon Nanotubes—Synthesis, Characterization, Applications*, ed. S. Yellampalli (InTech, 2011) <http://www.intechopen.com/books/carbon-nanotubes-synthesis-characterization-applications/dielectrophoretic-deposition-and-alignment-of-carbon-nanotubes>.  
doi: 10.5772/16487
- 39 R. Krupke, F. Hennrich, H. B. Weber, D. Beckmann, O. Hampe, S. Malik, M. M. Kappes, and H. V. Löhneysen: *Appl. Phys. A* **76** (2003) 397.
- 40 R. Krupke, F. Hennrich, H. V. Löhneysen, and M. M. Kappes: *Science* **301** (2003) 344.
- 41 Z. Xiao and F. E. Camino: *Nanotechnology* **20** (2009) 135205.
- 42 A. H. Monica, S. J. Papadakis, R. Osiander, and M. Paranjape: *Nanotechnology* **19** (2008) 085303.
- 43 E. F. Antunes, A. O. Lobo, E. J. Corat, and V. J. Trava-Airoldi: *Carbon* **45** (2007) 913.
- 44 L. C. Qin, Z. Liu, Q. Zhang, and H. Deniz: *Microsc. Microanal.* **13** (2007) 710.
- 45 J. Gigault, B. Grassl, I. L. Hécho, and G. Lespes: *Microchim. Acta* **175** (2011) 265.
- 46 R. Zou, J. Hu, Y. Song, N. Wang, H. Chen, H. Chen, J. Wu, Y. Sun, and Z. Chen: *J. Nanosci. Nanotechnol.* **10** (2010) 7876.
- 47 S. I. Rushfeldt: *Sensor Applications Carbon Nanotubes*, Master of Engineering Thesis, Materials Science and Engineering, Massachusetts Institute of Technology (2005) <http://dspace.mit.edu/handle/1721.1/33619>.
- 48 Y. A. Kim, T. Hayashi, M. Endo, and M. S. Dresselhaus: *Springer Handbook of Nanomaterials* (Springer, 2011).
- 49 N. J. Coville, S. D. Mhlanga, E. N. Nxumalo, and A. Shaikjee: *S. Afr. J. Sci.* **107** (2011) Art. #418.
- 50 L. Feng, N. Xie, and J. Zhong: *Materials* **7** (2014) 3919.
- 51 J. Jang and J. Bae: *Sens. Actuators, B* **122** (2007) 7.
- 52 B. Ding, M. Wang, J. Yu, and G. Sun: *Sensors* **9** (2009) 1609.
- 53 O. Monereo, S. Claramunt, M. Martínez de Marigorta, M. Boix, R. Leghrib, J. D. Prades, A. Cornet, P. Merino, C. Merino, and A. Cirera: *Talanta* **107** (2013) 239.
- 54 I. Kang, Y. Y. Heung, J. H. Kim, J. W. Lee, R. Gollapudi, S. Subramaniam, S. Narasimhadevara, D. Hurd, G. R. Kirikera, V. Shanov, M. J. Schulz, D. Shi, J. Boerio, and S. Mall, and M. Ruggles-Wren: *Composites Part B* **37** (2006) 382.
- 55 J.-M. Park, D.-S. Kim, S.-J. Kim, P.-G. Kim, D.-J. Yoon, and K. L. DeVries: *Composites Part B* **38** (2007) 847.
- 56 D. D. L. Chung: *Carbon* **50** (2012) 3342.
- 57 M. Ge and K. Sattler: *Chem. Phys. Lett.* **220** (1994) 192.
- 58 R. Zheng, Y. Zhao, H. Liu, C. Liang, and G. Cheng: *Carbon* **44** (2006) 742.
- 59 B. O. Lee, W. J. Woo, and M. S. Kim: *Macromol. Mater. Eng.* **286** (2001) 114.
- 60 E. Hammel, X. Tang, M. Trampert, T. Schmitt, K. Mauthner, and A. Eder: *Carbon* **42** (2004) 1153.
- 61 K. Mukhopadhyay, D. Porwal, D. Lal, K. Ram, and G. N. Mathur: *Carbon* **42** (2004) 3254.
- 62 W. Brandl, G. Marginean, V. Chirila, and W. Warschewski: *Carbon* **42** (2004) 5.
- 63 V. Z. Mordkovich: *Theor. Found. Chem. Eng.* **37** (2003) 429.
- 64 K. Lozano: *JOM* **52** (2000) 34.
- 65 M. H. Al-Saleh and U. Sundararaj: *Carbon* **47** (2009) 2.
- 66 M. Inagaki, Y. Yang, and F. Kang: *Adv. Mater.* **24** (2012) 2547.
- 67 L. Zhang, A. Aboagye, A. Kelkar, C. Lai, and H. Fong: *J. Mater. Sci.* **49** (2014) 463.
- 68 G. C. Rutledge and S. V. Fridrikh: *Adv. Drug Delivery Rev.* **59** (2007) 1384.
- 69 A. L. Yarin, S. Koombhongse, and D. H. Renekers: *J. Appl. Phys.* **90** (2001) 4836.
- 70 X. Mao, T. Hatton, and G. Rutledge: *Curr. Org. Chem.* **17** (2013) 1390.
- 71 I. M. Alarifi, A. Alharbi, W. S. Khan, A. Swindle, and R. Asmatulu: *Materials* **8** (2015) 7017.
- 72 S. Parveen, S. Rana, and R. Fanguero: *J. Nanomater.* **2013** (2013) 710175.
- 73 P. Carballeira: *Mechanical and Electrical Properties of Carbon Nanofiber–Ceramic Nanoparticle–Polymer Composites*, Doctoral Thesis, Institut für Verbundwerkstoffe GmbH (IVW), Technical University Kaiserslautern (2010).

- 74 E. Zussman, X. Chen, W. Ding, L. Calabri, D. A. Dikin, J. P. Quintana, and R. S. Ruoff: *Carbon* **43** (2005) 2175.
- 75 B. Zhang, F. Kang, J.-M. Tarascon, and J.-K. Kim: *Prog. Mater. Sci.* **76** (2016) 319.
- 76 P. Kim, L. Shi, A. Majumdar, and P. L. McEuen: *Phys. Rev. Lett.* **87** (2001) 2155021.
- 77 M. J. Madou: *From MEMS to Bio-MEMS and Bio-NEMS: Manufacturing Techniques and Applications* (CRC Press, 2011) p. 650.
- 78 M. Law, J. Goldberger, and P. Yang: *Annu. Rev. Mater. Res.* **34** (2004) 83.
- 79 X. Zhao, Y. Ando, Y. Liu, M. Jinno, and T. Suzuki: *Phys. Rev. Lett.* **90** (2003) 187401.
- 80 M. F. L. De Volder, R. Vansweevelt, P. Wagner, D. Reynaerts, C. Van Hoof, and A. J. Hart: *ACS Nano* **5** (2011) 6593.
- 81 A. Amma, B. Razavi, S. K. St. Angelo, T. S. Mayer, and T. E. Mallouk: *Adv. Funct. Mater.* **13** (2003) 365.
- 82 A. M. Zaitsev, A. M. Levin, and S. H. Zaidi: *IEEE Sens. J.* **8** (2008) 849.
- 83 A. M. Zaitsev, A. M. Levin, and S. H. Zaidi: *Phys. Stat. Sol., A* **204** (2007) 3574.
- 84 P. Philipp: *Phase Transformation in Tetrahedral Amorphous Carbon by Focused Ion Beam Irradiation*, Doctor Thesis, Faculty of Mathematics and Natural Sciences, Technical University Dresden (2014).
- 85 <http://www.nanowerk.com/spotlight/spotid=11804.php> (accessed 30 January 2016).
- 86 B. Mahar, C. Laslau, R. Yip, and Y. Sun: *IEEE Sens. J.* **7** (2007) 266.
- 87 H. Chiu, P. Hung, H. W. Ch. Postma, and M. Bockrath: *Nano Lett.* **8** (2008) 4342.
- 88 B. H. Son, J. Park, S. Lee, and Y. H. Ahn: *Nanoscale* **7** (2015) 15421.
- 89 J. Lee, A. B. Kaul, and P. X.-L. Feng: "Vertical Carbon Nanofiber Arrays and Nanomechanical Resonators with Potential for Radiation Sensing", *Digest of Tech. Papers, the 17th International Conference on Solid-State Sensors, Actuators and Microsystems (Transducers 2013)*, 1887–1890, Barcelona, Spain, June 16–20 (2013).
- 90 A. B. Kaul: *2012 IEEE Int. Frequency Control Symp.* (2012) pp. 1–4.
- 91 J. Heo, M. Madou, and H. Shin: *15th International Conference on Miniaturized Systems for Chemistry and Life Sciences*, October 2–6, 2011, Seattle, Washington, USA (2011) pp. 1971–1973.
- 92 D. Saini, H. Behlow, R. Podila, D. Dickel, B. Pillai, M. J. Skove, S. M. Serkiz, and A. M. Rao: *Sci. Rep.* **4** (2014) 5542.